Brugada syndrome and fever: Genetic and molecular characterization of patients carrying *SCN5A* mutations

Dagmar I. Keller[a,c,e,1], Jean-Sébastien Rougier[b,1], Jan P. Kucera[d], Nawal Benammar[f], Véronique Fressart[f], Pascale Guicheney[e], Alois Madle[g], Martin Fromer[a], Jürg Schläpfer[a,*], Hugues Abriel[a,b,*]

[a]*Service of Cardiology, CHUV, Lausanne, Switzerland*
[b]*Department of Pharmacology and Toxicology, University of Lausanne, Switzerland*
[c]*Department of Cardiology, University Hospital, Basel, Switzerland*
[d]*Department of Physiology, University of Bern, Switzerland*
[e]*INSERM U582, Institut de Myologie, IFR14, Pitié-Salpêtrière Hospital, Paris, France*
[f]*Service of Biochemistry B, IFR 14, Pitié-Salpêtrière Hospital, Paris, France*
[g]*Second Department of Medicine, University Hospital, 30599 Pilzen, Czech Republic*

Abstract

Objective: Brugada syndrome (BrS) is characterized by ventricular tachyarrhythmias leading to sudden cardiac death and is caused, in part, by mutations in the *SCN5A* gene encoding the sodium channel Na$_v$1.5. Fever can trigger or exacerbate the clinical manifestations of BrS. The aim of this work was to characterize the genetic and molecular determinants of fever-dependent BrS.

Methods: Four male patients with typical BrS ST-segment elevation in V1–V3 or ventricular arrhythmias during fever were screened for mutations in the *SCN5A* gene. Wild-type (WT) and mutant Na$_v$1.5 channels were expressed in HEK293 cells. The sodium currents (I_{Na}) were analysed using the whole-cell patch clamp technique at various temperatures. Protein expression of WT and mutant channels was studied by Western blot experiments.

Results: Two mutations in *SCN5A*, L325R and R535X, were identified. Expression of the two mutant Na$_v$1.5 channels in HEK293 cells revealed in each case a severe loss-of-function. Upon the increase of temperature up to 42 °C, we observed a pronounced acceleration of Na$_v$1.5 activation and fast inactivation kinetics. Cardiac action potential modelling experiments suggest that in patients with reduced I_{Na}, fever could prematurely shorten the action potential by virtue of its effect on WT channels. Further experiments revealed that L325R channels are likely misfolded, since their function could be partially rescued by mexiletine or curcumin. In co-expression experiments, L325R channels interfered with the proper function of WT channels, suggesting that a dominant negative phenomenon may underlie BrS triggered by fever.

Conclusions: The genetic background of BrS patients sensitive to fever is heterogeneous. Our experimental data suggest that the clinical manifestations of fever-exacerbated BrS may not be mutation specific.

---

* Corresponding authors. H. Abriel is to be contacted at Service of Cardiology, and Department of Pharmacology and Toxicology, University of Lausanne, Bugnon, 27, 1005 Lausanne, Switzerland. Tel.: +41 21 6925364; fax: +41 21 6935355. J. Schläpfer, Service of Cardiology, CHUV and University of Lausanne, 1011 Lausanne, Switzerland. Tel.: +41 21 3140052; fax: +41 21 3140013.

E-mail addresses: Jurg.Schlaepfer@chuv.hospvd.ch (J. Schläpfer), Hugues.Abriel@unil.ch (H. Abriel).

[1] Both authors contributed equally to this study.

1. Introduction

Brugada syndrome (BrS) is characterized by ST segment elevation in the right precordial leads V1–V3 on the surface ECG, with incomplete or complete right bundle branch block and an increased risk for sudden cardiac death (SCD) caused by polymorphic ventricular tachycardia or fibrillation (VT/VF) [1]. The BrS is a primary electrical cardiac disorder with no apparent underlying structural heart disease and is inherited by an autosomal dominant trait. Mutations have been identified in the *SCN5A* gene encoding the α-subunit of the voltage-gated sodium channel $Na_v1.5$ [2]. Yet, only 10–30% of clinically affected individuals carry a mutation in this gene [3]. Most of *SCN5A* mutations lead to a "loss-of-function" by reducing the sodium current (I_{Na}) available during the phases 0 (upstroke) and 1 (early repolarization) of the cardiac action potential (AP) [1].

The molecular and cellular mechanisms leading to the BrS are not yet completely understood. In some patients, the BrS is concealed on the surface ECG and can be unmasked using sodium channel blockers. Furthermore, fever has been reported to unmask or exacerbate the typical BrS ECG pattern on the surface ECG and to trigger VT [4]. During the past six years, several case reports of fever-induced BrS have been published [5–9].

In the present study, we screened *SCN5A* in four unrelated patients presenting typical BrS ECGs during episodes of fever. Two heterozygous mutations were identified: a novel missense mutation, L325R, and a nonsense mutation, R535X. We carried out molecular and functional analyses of the consequences of these two mutations, using classical biochemical and patch-clamp techniques. The two mutations markedly decreased the I_{Na} after transfection of the mutant proteins, suggesting that reduced availability of I_{Na} during the early phase of the cardiac AP may cause fever-induced tachyarrhythmias. We also provide experimental evidence for protein misfolding resulting from the L325R mutation, since the I_{Na} mediated by these mutant channels was partially rescued by curcumin and mexiletine. In addition, we present data suggesting for the first time that BrS mutant channels may exert a dominant negative effect on WT channels.

2. Methods

This study was performed according to the guidelines of the Swiss Society of Medical Genetics and conforms to the Declaration of Helsinki. All individuals gave written informed consent to participate in the study.

2.1. Molecular screening

Genomic DNA was extracted from peripheral lymphocytes. In the four patients, the coding exons of *SCN5A* were amplified by polymerase chain reaction (PCR), using primers designed in intronic flanking sequences, according to the gene sequences [10]. Denaturing high performance liquid chromatography (DHPLC) was performed on DNA-amplification products in at least one temperature condition. Abnormal DHPLC profiles were analysed by sequence reaction in both strands of the exon, using big dye termination mix, and analysed by cycle sequencing on an automated laser fluorescent DNA sequencer (ABI prism 3100, Applied Biosystems). The novel mutation L325R was absent in 200 normal alleles.

2.2. Functional and biochemical analysis of Na^+ channels

SCN5A mutations were engineered into WT cDNA (clone hH1a received from Dr. R. Kass) cloned in pcDNA3.1 (Invitrogen), using the QuickChange Kit (Stratagene) and verified by sequencing. For electrophysiology studies, HEK293 cells were transiently transfected with 0.6 μg WT or mutant $Na_v1.5$ construct cDNAs or as indicated. All transfections included 2.0 μg pIRES-hβ1-CD8 cDNA encoding hβ1 subunit and CD8 antigen, as a reporter gene. Cells were transfected using calcium phosphate and I_{Na} were measured after 48 h. Anti-CD8 beads (Dynal) were used to identify transfected cells. Patch-clamp recordings were carried-out using an internal solution containing (mmol/L) CsCl 60; Cs Aspartate 70; EGTA 11; MgCl$_2$ 1; CaCl$_2$ 1; HEPES 10; and Na$_2$-ATP 5, pH 7.2 with CsOH; external solution NaCl 130; CaCl$_2$ 2; MgCl$_2$ 1.2; CsCl 5; HEPES 10; and glucose 5, pH 7.4 with CsOH. Using these solutions, 5 min after rupturing the membrane, we observed no significant alteration of the availability curve and the peak current. Holding potentials were −100 mV and no leak subtraction was performed. Peak currents were measured during a current-voltage protocol and I_{Na} densities (pA/pF) were obtained by dividing the peak I_{Na} by the cell capacitance obtained from the pClamp function. Measurements were carried out at different temperatures using a control system (Cell MicroControls) heating the perfusion solution. Obtaining an adequate voltage-clamp control when measuring voltage-gated I_{Na} in voltage-clamp conditions at physiological temperatures may represent a difficult task. We took great care to ensure the best possible voltage-clamp control: (1) We compensated the series resistances by virtually 100% using a VE-2 amplifier (Alembic Instruments) based on a "state estimator" series resistance compensation approach [11]. (2) The resistance of the pipettes was in the range of 1.7–2.5 MΩ. (3) We used data only from cells where the access resistance remained stable over all the duration of the experiment. (4) Cells for which signs of poor voltage-clamp control such as delayed inflections of the current or discontinuities in the peak I_{Na} vs. Vm curve were not analysed. As presented in the Table 1, despite the fact that activation kinetics were faster with increasing temperature (22 °C up to 42 °C, see Fig. 4) the voltage dependence of activation characterized by the $V_{1/2}$ of activation and, most importantly, the slope factor K were

Table 1
The following biophysical parameters of WT and L325R channels were recorded at 22, 37 and 42 °C: $V_{1/2}$ values and slope factor (K) of the voltage-dependence of steady-state activation and inactivation

		22 °C		37 °C		42 °C	
Activation							
K (mV/e-fold)	WT	5.4 ± 0.4 ($n=9$)		4.9 ± 0.4 ($n=6$)		5.3 ± 0.2 ($n=5$)	
	L325R	7.2 ± 0.3 ($n=7$)	*	7.9 ± 0.3 ($n=4$)	*	8.4 ± 1.0 ($n=4$)	*
$V_{1/2}$ (mV)	WT	-41.0 ± 2.3 ($n=9$)		-42.8 ± 1.7 ($n=6$)		-42.0 ± 2.3 ($n=5$)	
	L325R	-31.0 ± 1.1 ($n=7$)	**	-32.4 ± 3.5 ($n=4$)	*	-33.3 ± 1.7 ($n=4$)	*
Time to the peak (ms)	WT	0.49 ± 0.03 ($n=9$)		0.35 ± 0.06 ($n=5$)	#	0.36 ± 0.07 ($n=5$)	#
	L325R	0.71 ± 0.03 ($n=7$)	***	0.47 ± 0.02 ($n=4$)	n.s. ###	0.43 ± 0.04 ($n=4$)	n.s. ###
Inactivation							
K (mV/e-fold)	WT	6.1 ± 0.3 ($n=5$)		5.8 ± 0.4 ($n=5$)		5.5 ± 0.3 ($n=5$)	
	L325R	5.9 ± 0.2 ($n=18$)	n.s.	4.9 ± 0.3 ($n=9$)	n.s.	5.5 ± 0.7 ($n=8$)	n.s.
$V_{1/2}$ (mV)	WT	-77.1 ± 1.6 ($n=5$)		-77.7 ± 1.9 ($n=5$)		-77.9 ± 2.3 ($n=5$)	
	L325R	-74.0 ± 1.0 ($n=18$)	n.s.	-73.3 ± 1.6 ($n=12$)	n.s.	-71.3 ± 0.9 ($n=8$)	**
τ (ms)	WT	0.52 ± 0.02 ($n=7$)		0.29 ± 0.02 ($n=3$)	###	0.25 ± 0.02 ($n=3$)	###
	L325R	0.84 ± 0.05 ($n=7$)	***	0.58 ± 0.05 ($n=4$)	** ##	0.60 ± 0.04 ($n=4$)	** #
I_{Na} amplitude (%)	WT	100 ± 19 ($n=11$)		118 ± 3 ($n=9$)	###	116 ± 4 ($n=6$)	##
	L325R	100 ± 10 ($n=14$)		119 ± 4 ($n=8$)	###	124 ± 8 ($n=5$)	##

Steady-state inactivation protocol used: 25-ms test pulse to -20 mV after a 500-ms conditioning pulse. The data from individual cells were fitted with Boltzmann relationship, $y(Vm)=1/(1+\exp[(Vm-V_{1/2})/K])$, in which y is the normalized current or conductance, Vm is the membrane potential, $V_{1/2}$ is the voltage at which half of the channels are activated or inactivated, and K is the slope factor.
Mean time to the peak I_{Na}, time constant (τ) of onset of fast inactivation, and normalized peak I_{Na} were all measured at -20 mV, number of cells in parenthesis; *, **, ***$p<0.05$, 0.01, 0.001 vs. WT; #, ##, ###$p<0.05$, 0.01, 0.001 vs. 22 °C respectively; n.s. not significant vs. WT.

not significantly influenced by the temperature, indicating that the quality of the voltage-clamp control was comparable at all temperatures tested. In some experiments, cells were pre-incubated with thapsigargin (Acros), curcumin (Acros), or mexiletine (Sigma). The cells were washed of the drugs 10 min prior to the recordings.

Western blotting conditions have been described previously [12]. The anti-Na$_v$1.5 affinity purified antibody recognizes residues 493–511 of rat Na$_v$1.5 (ASC-005, Alomone). These residues are identical in the human sequence. Anti-actin antibody was from Sigma.

Data are presented as means±SEM. Two-tailed Student t-test was used to compare means; $p<0.05$ was considered significant.

2.3. Mathematical modelling of I_{Na} and of the action potential

WT I_{Na} was modelled using the 6-state Markovian model of Clancy and Rudy [13] (errata on http://rudylab.wustl.edu/research/cell/methodology/markov/ina.htm). Temperature-dependence of the transition rates was incorporated using a Q_{10} factor approach according to the following equation: $\alpha(T)=Q_{10}^{(T-T_0)/10}\cdot\alpha(T_0)$, where T is absolute temperature, $\alpha(T)$ is the rate at temperature T, and $\alpha(T_0)$ the original model rate at the reference temperature T_0 of 310.15 °K. To reconstruct the AP of the right ventricular epicardium, this I_{Na} formulation was introduced into the Luo–Rudy dynamic (LRd) cell model [14], with the updates proposed by Faber [15]. As done previously [16], the transient outward K$^+$ current (I_{to}) was incorporated according to Dumaine et al. [17] with a maximal conductance of 1.35 mS/μF to simulate the high I_{to} density in the right ventricular epicardium. The AP was elicited by a 0.5 ms current pulse of 80 μA/μF.

3. Results

3.1. Description of four index cases with fever-sensitive BrS

This study included four male index cases of Caucasian origin in whom either typical BrS ECG pattern and/or VT was triggered by fever. Patient 1, 44-year-old, was admitted in the emergency room for investigation of a first episode of syncope during fever (up to 39 °C) caused by pneumonia. The ECG was suggestive of BrS (Fig. 1) and an ajmaline test was positive. No sustained ventricular arrhythmia was inducible during electrophysiological study (EPS). The patient received an implantable cardioverter defibrillator (ICD). Patient 2, 57-year-old, was referred for investigation of syncope while driving resulting in a car accident. Resting ECG showed clear ST segment elevation in V1–V2 compatible with BrS, and an ICD was implanted (Fig. 1). During three fever episodes due to pneumonia, the patient had several sustained VT episodes successfully terminated by the ICD. Patient 3, a 45-year-old subject with no previous history of syncope, was admitted at the hospital for bacterial enteritis with fever (39.8 °C). The routine ECG showed a typical BrS pattern (Fig. 1). Two days later, when the patient was afebrile, the ECG was normalized. A flecainide test was positive, but no ventricular arrhythmia was inducible during EPS. The clinical presentation of the fourth patient, a 50-year-old

Index Case 1 ECG (38.0°C, pneumonia) **Index Case 2 ECG (rest, no fever)**

Index Case 3 ECG (39.8°C, enteritis) **Index Case 4 ECG (38.1°C, pleuritis)**
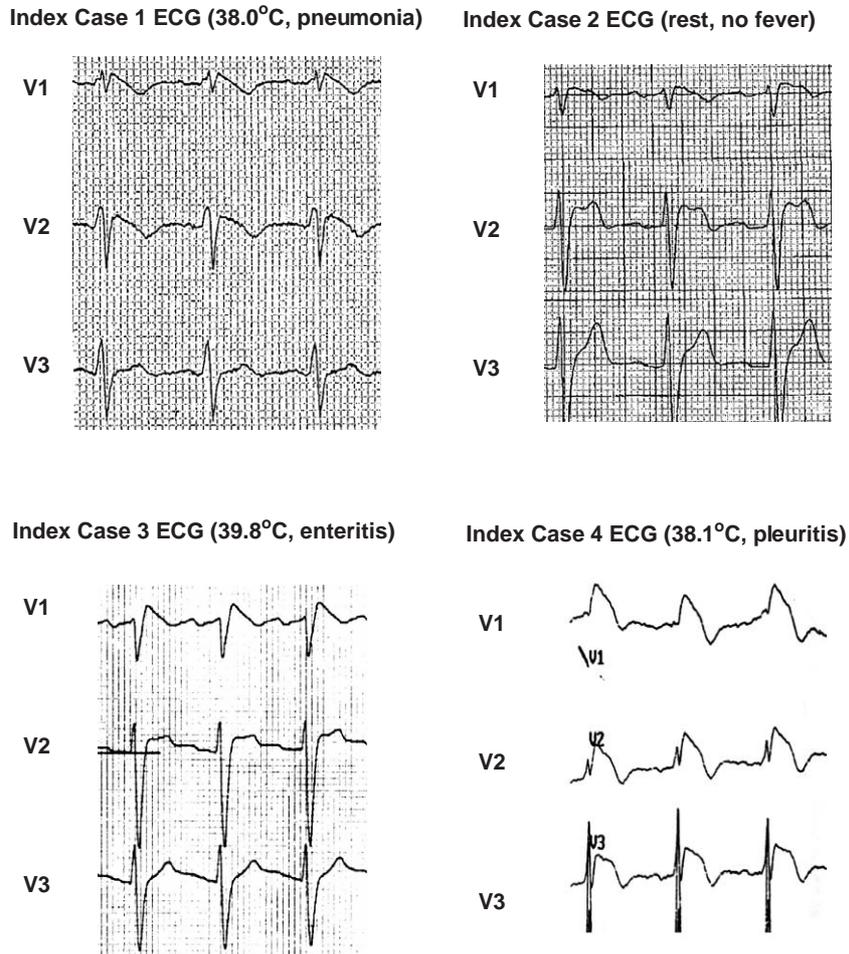
Fig. 1. Electrocardiograms of the four unrelated index cases showing different BrS patterns in leads V1–V3. The index cases 1–3 are patients followed at the University Hospital of Lausanne (Switzerland). Patient 4 originated from Pilzen (Czech Republic).

male, has been previously published [5]. Briefly, the patient was admitted at the hospital with pleuritis and fever (38.1 °C). The ECG showed downward sloping ST segment elevations in V1–V3 and was normalized as soon as the patient was afebrile. However, a similar abnormal ECG was recorded after infusion of ajmaline. Only patient 3 had a family history of SCD; his half-brother died suddenly at age 48 for an unknown reason, with no demonstrable heart disease.

3.2. Identification of two SCN5A mutations

We screened all coding exons of *SCN5A* by a PCR-DHPLC-sequencing approach. A novel heterozygous missense mutation was identified in patient 2. A T to G substitution at position 974 resulted in the L325R mutation with a positively charged arginine (Fig. 2A). The leucine-325 residue is located in the linker segment preceding the domain 1 P-loop (Fig. 2C). In patient 3, a heterozygous non-sense mutation was identified, R535X, resulting from a C to T substitution at position 1603. This mutation leads to a premature stop codon (Fig. 2B) and has been

previously described [18]. However, an investigation of the functional consequences of this mutation has not been performed, yet.

3.3. Electrophysiological characterization of the two mutant Na$_v$1.5 channels

The functional consequences of the *SCN5A* mutations were studied, using HEK293 cells transiently transfected with mutant cDNAs. As illustrated in Fig. 3A, the level of expression of the L325R mutant channels analysed by Western blot was comparable to that of WT channels. In contrast, using the patch-clamp technique, L325R channels generated I_{Na} that was reduced by about 80%, compared to WT channels (Fig. 3B–C). At room temperature (22 °C), the steady-state inactivation parameters of L325R channels were not different from WT (Table 1). In contrast, the L325R mutation caused a ~10 mV positive shift of the $V_{1/2}$ steady-state activation curve (Table 1). Kinetics of activation (assessed by the time to the peak) and onset of fast inactivation were slower for the L325R I_{Na} (Table 1 and Fig. 4A).
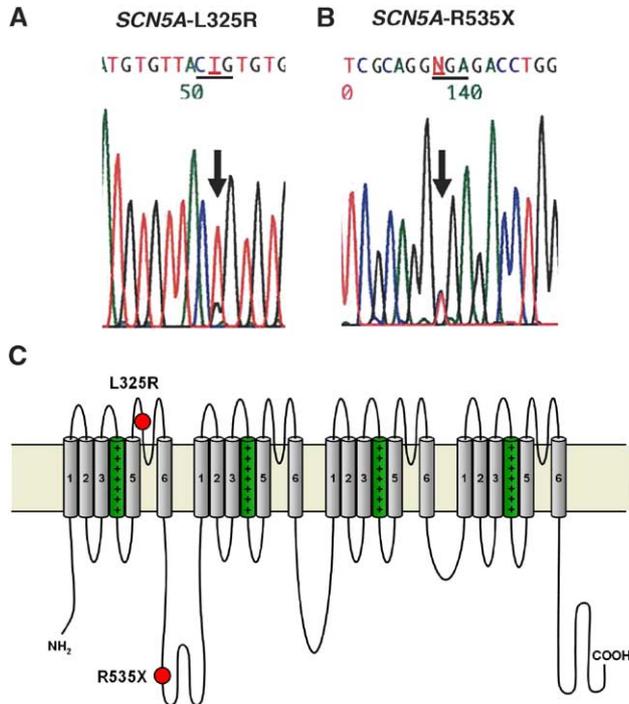
Fig. 2. Genetic analysis of the two index cases with *SCN5A* mutations. (A and B) Sequence analysis of *SCN5A* exons 8 and 12 with base changes leading to the L325R and R535X mutations in index cases 2 (A) and 3 (B), respectively. (C) Membrane topology of $Na_v1.5$ and the location of the two mutations (circles).

Transient expression of R535X channels yielded a truncated protein with a molecular weight which, as predicted from the sequence, was about one fourth of that of the WT protein (Fig. 3D). No I_{Na} could be recorded from cells expressing the truncated protein (Fig. 3E–F).

3.4. Effect of temperature on the properties of WT and L325R channels and on the action potential

In order to get further insight into the mechanisms underlying the effect of fever, we analysed the effect of temperature on WT and L325R channels. Data presented in the Table 1 (and see Methods) illustrates that we achieved an excellent voltage-clamp control for the recording of I_{Na} at physiological temperatures. Increasing the temperature significantly accelerated both the activation and inactivation kinetics of WT and L325R I_{Na} (Fig. 4A and Table 1) and, in agreement with a previous study [19], the resultant peak I_{Na} was increased. The peak WT I_{Na} was $16\pm4\%$ larger at 42 °C compared to 22 °C; L325R I_{Na} was increased by $24\pm8\%$. The steady-state inactivation and activation parameters were also measured at 37 °C and 42 °C and the difference in activation $V_{1/2}$ that was observed at room temperature was still present (Table 1). No significant temperature-dependence of both $V_{1/2}$ and K-slope factor was observed, neither for activation, nor for inactivation.

How to explain the increase in peak I_{Na} paralleling the increasing temperature? If one assumes that all kinetic

processes governing I_{Na} follow an identical sensitivity to temperature (Q_{10} factor), one would expect I_{Na} to exhibit an overall accelerated time course without any major change of its peak. This increase of peak I_{Na} could thus be the consequence of a Q_{10}, which is larger for activation than for inactivation, leading to a relatively larger acceleration of activation, compared to inactivation. To test this hypothesis, we used, in a first step, a Hodgkin–Huxley formalism to estimate Q_{10} for activation and inactivation by fitting WT I_{Na} recordings elicited by pulses to -10 mV with the function $I_{Na}=gNa_{max}.(1-\exp(-\alpha_m t))^3.(\exp(-\alpha_h t)).$ $(V-E_{Na})$, where α_m and α_h are the rate constants for activation and inactivation, respectively. Then, the Q_{10} factors were computed from the slope of the linear regression of $\ln(\alpha_m)$ and $\ln(\alpha_h)$ as a function of temperature. Q_{10} values of 2.11 ($r=0.97$) and 1.90 ($r=0.99$) were obtained for α_m and α_h, respectively. In a second step, we
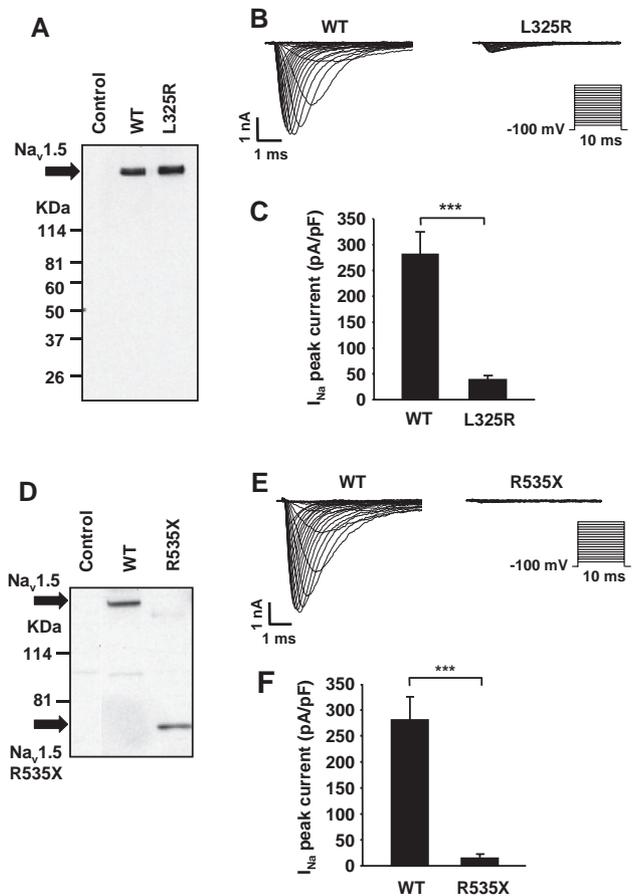
Fig. 3. Biochemical and functional analysis of L325R and R535X mutant channels. (A) Western blot of HEK293 cell lysates expressing WT and L325R channels. Controls are non-transfected cells. (B) Current traces recorded from cells expressing WT or L325R channels in response to a series of 10-ms test pulses (inset). (C) Averaged peak currents of cells expressing WT and L325R channels, $n=15$ cells from 3 independent experiments, ***$p<0.001$. (D) Western blot of cells expressing WT and R535X mutant proteins. (E) Current traces recorded from cells expressing WT or R535X channels. (F) Averaged peak currents of cells expressing WT and R535X channels, $n=15$ cells from 3 independent experiments, ***$p<0.001$.
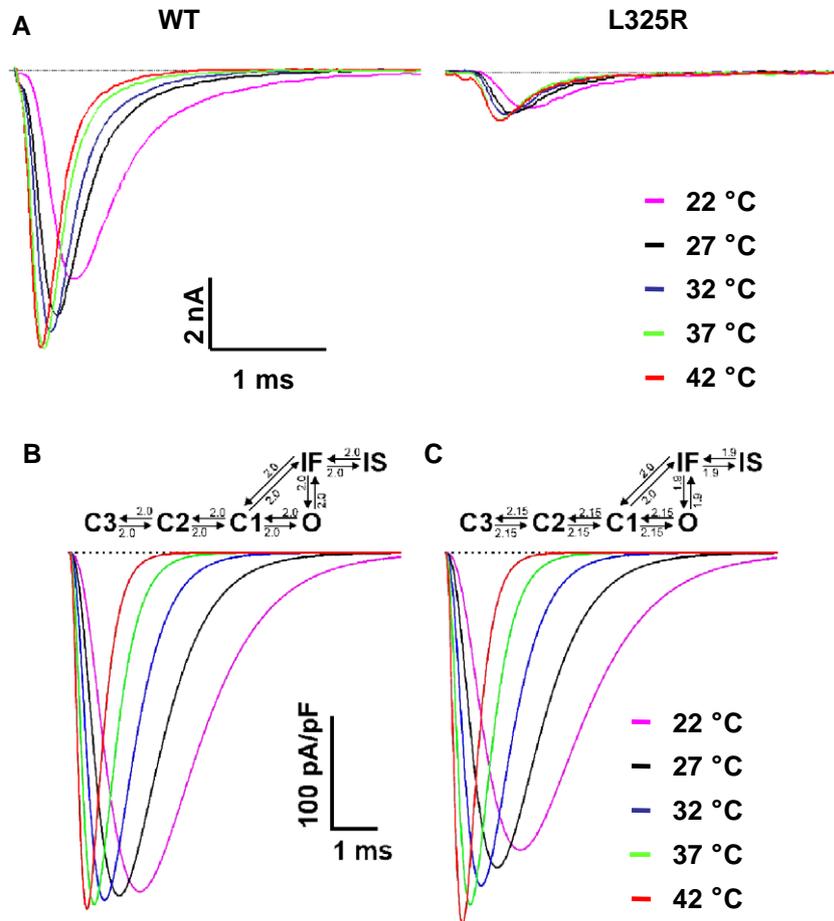
Fig. 4. I_{Na} recordings of WT and L325R channels at different temperatures, and mathematical modelling. (A) Representative current traces obtained after depolarizing HEK293 cells expressing WT or L325R channels at −20 mV (holding potential −100 mV) at different temperatures. (B and C) Reconstruction of WT I_{Na}, using the Clancy–Rudy model under the assumption of an identical Q_{10} of 2.0 for all transition rates (B) and of a Q_{10} that is larger for activation rates compared to inactivation rates (2.15 vs. 1.9, C). The Q_{10} used are marked on the respective state transition diagrams. The voltage-clamp protocol is the same as in (A).

reconstructed I_{Na}, as shown in Fig. 4B and C, using a Markovian model of the WT channel [13], in which we incorporated temperature-dependence using the Q_{10} formalism. When we assumed Q_{10} to be identical for all rate constants (the value of 2.0 was chosen between 2.1 and 1.9), increasing temperature from 22 to 42 °C resulted only in a modest peak I_{Na} increase of 5.2% (Fig. 4B). In the simulation presented in Fig. 4C, we incorporated Q_{10} values of 2.15 for all three activation transitions and 1.9 for both inactivation transitions. The absence of a temperature-dependence of $V_{1/2}$ for steady-state activation and availability in our experiments indicates that there is no change in the steady-state occupancy of the different states with increasing temperature. Consequently, this suggests that for a given transition, the ratio of the forward and backward rates does not change with temperature. Therefore, the Q_{10}'s for the reverse transitions (deactivation and recovery from inactivation, respectively) were set equal to that of the forward transitions. The Q_{10}'s for the transition between states IF and C1 could not be determined from our experiments and an intermediate value of 2.0 was assumed

in both directions. Using this set of Q_{10} parameters, peak I_{Na} increased by 24.8% when temperature was increased from 22 to 42 °C (Fig. 4C), an increase which is similar to that observed experimentally. The effects of this temperature-dependent behaviour of WT I_{Na} on the right ventricular epicardial AP were further investigated using the LRd model (Fig. 5). In the control simulation (100% I_{Na}, 37 °C, Fig. 5A), the AP exhibited a deep notch characteristic of the right ventricular AP. No significant changes in AP morphology were observed when either temperature was increased to 40 °C (Fig. 5B) or when I_{Na} was reduced to 50% to simulate a heterozygote BrS mutant cell (Fig. 5C). However, with 50% I_{Na} and at 40 °C, the AP exhibited premature repolarization and a loss of the dome, consistent with the cellular model of BrS (Fig. 5D).

3.5. Rescue of the L325R Na$_v$1.5 currents

The large decrease in peak current density caused by the L325R mutation (about 80%) cannot be explained by the alterations in the biophysical properties of L325R Na$_v$1.5.
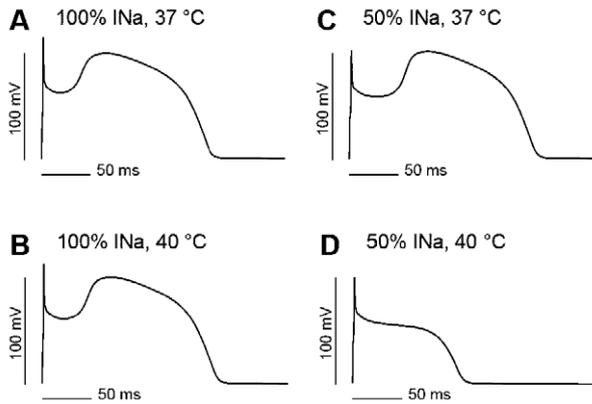
Fig. 5. Mathematical modelling of the AP using the temperature-dependent I_{Na} model presented in Fig. 4C. (A) Control AP (at 37 °C and with 100% I_{Na}). (B) Simulation of increased temperature (40 °C, with 100% I_{Na}). (C) Simulation with 50% I_{Na}, mimicking a heterozygote genotype, at 37 °C. (D) Simulation with 50% I_{Na} and at 40 °C. Note the abbreviation of the AP and the loss of the dome.

Because the mutation replaces an uncharged leucine by a positively charged arginine, we considered the hypothesis that this mutation influences the folding process of the protein, thus altering either biosynthesis or trafficking of the channel. Fig. 6A illustrates that, similarly to a recent report [20], pre-incubation of the cells expressing L325R channels with 500 μM mexiletine rescued the mutant I_{Na} up to 55% of the WT current. We also investigated the effect of curcumin, which has been shown to rescue misfolded mutant CFTR channels in a mouse model of cystic fibrosis [21]. This drug is a low-toxic sarcoplasmic reticulum Ca^{2+}-ATPase inhibitor [22]. Incubation with 25 μM of curcumin during 24 h increased significantly the mutant currents by ~150% (Fig. 6A). In contrast, thapsigargin, another drug known to rescue certain misfolded ion channels [23], had no effect. In addition to these treatments expected to improve trafficking of misfolded channels, we also incubated cells expressing L325R channels for 24 h at 28 °C. This condition also partially rescued the mutant channels by ~300% (Fig. 6A).

3.6. Dominant negative effect of the L325R mutant allele

Consistent with an autosomal dominant trait, both *SCN5A* mutation carriers were found to be heterozygous. In order to mimic this state in our cellular model, we investigated the co-expression of WT and mutant "alleles" by co-transfecting WT and mutant cDNAs. Fig. 6B shows that when reducing the amount of WT cDNA by 50%, the resultant I_{Na} was decreased by about 50%. This condition represents the clinical situation were there would be no synthesis at all of the protein resulting from the mutant allele. However in our experimental model, both mutants were expressed (Fig. 3A and D). When WT and L325R channels were co-transfected in a 1:1 ratio, the peak I_{Na} was reduced to only $18 \pm 8\%$ of the control condition where

100% of WT channels were expressed (Fig. 6B). This finding strongly suggests that the L325R allele exerts a dominant negative effect on WT channels. In contrast, this negative effect was not observed when the truncated R535X
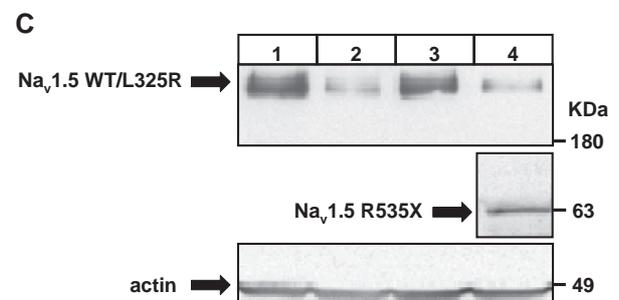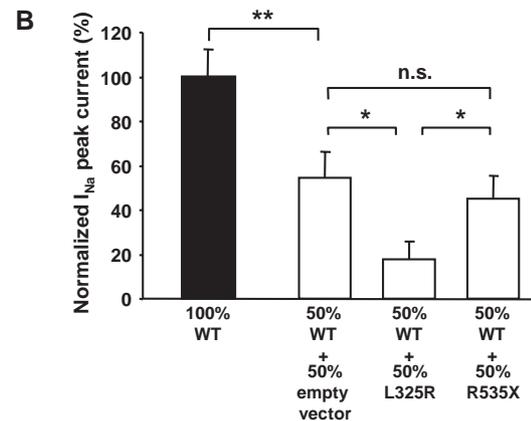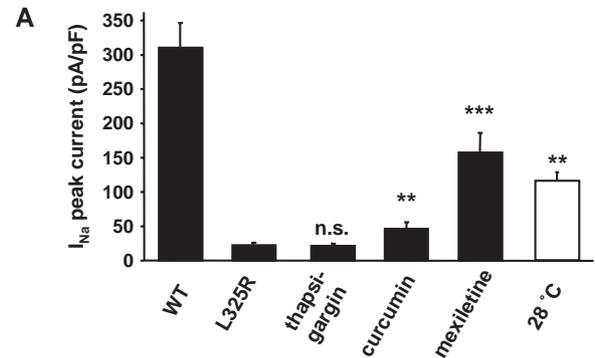
Fig. 6. Treatments rescuing L325R channels and dominant negative effect of L325R channels. (A) HEK293 cells were transfected with WT or L325R cDNAs and I_{Na} was measured after 48 h. L325R cells were treated with either thapsigargin 1 μM for 12 h, curcumin 25 μM for 24 h, or mexiletine 500 μM for 24 h, or incubated for 24 h at 28 °C; $n = 15–20$ cells from at least 2 independent experiments, **$p < 0.01$, ***$p < 0.001$ vs. L325R. (B) HEK293 cells were transfected with WT and mutant cDNAs. 100% corresponds to 0.3 μg cDNA per transfection flasks. In the second condition, the WT cDNA was reduced to 50% (0.15 μg cDNA) and complemented with empty cDNA vector. The condition mimicking the heterozygous expression of WT and mutant channels revealed an interference of the L325R proteins with the current generated by the WT channels. The R535X protein had no negative influence on the WT currents; $n = 15–20$ cells from at least 3 independent experiments, *$p < 0.05$, **$p < 0.01$. (C) Western blots of HEK293 cell lysates illustrating the levels of expression of WT and mutant channels in the four conditions analysed in (B). Protein loading was verified by anti-actin immunoblotting.

and the WT proteins were co-transfected (Fig. 6B). Since, the total pool of expressed $Na_v1.5$ proteins is unchanged (Fig. 6C), it can be postulated that the L325R channels interfere with the trafficking of WT channels.

4. Discussion

In this study, we identified two mutations in the *SCN5A* gene in four index patients with BrS pattern ECGs during episodes of fever. Our in vitro data indicate that the mutations cause an important loss-of-function of the $Na_v1.5$ channels. Functional analyses of the L325R and R535X mutant channels suggest that the manifestations of fever-exacerbated BrS may not be mutation specific. Furthermore, our experiments suggest novel molecular mechanisms underlying BrS, such as misfolding of mutant proteins leading to dominant negative effect of mutant channels.

4.1. Clinical and genetic findings

Fever can trigger VT/VF in BrS patients [4]. Here, we report four male cases in which *SCN5A* has been screened. Two mutations were found; R535X in an asymptomatic patient with a typical BrS ECC pattern during fever and L325R, a novel mutation, in a patient with fever-induced VT. The main clinical implications of these findings are that BrS has to be considered in patients with unexplained syncope during febrile state, and that genetic investigation should be performed in patients with an ECG suggestive of BrS during fever. Finally, BrS patients should be advised to take antipyretic drugs early in the course of any febrile illness.

4.2. Possible mechanisms of fever susceptibility in BrS patients

One of the current models explaining the ECG alterations seen in BrS is based on an imbalance between the depolarizing and repolarizing currents during the AP phase 1, mainly in cells expressing a large transient outward I_{to} current as the epicardial cells of the right ventricle [1]. In patients with loss-of-function mutations of $Na_v1.5$, resulting in less I_{Na} during the phase 1, the large I_{to} current may repolarize the membrane prematurely producing a loss of the dome (phase 2) of the AP. When such premature AP shortening happens heterogeneously in the myocardium, this may generate phase 2 re-entries that can cause VT/VF. Hence, the delicate balance of currents, mainly I_{to} (repolarizing), I_{Ca} and I_{Na} (both depolarizing), during the AP phase 1 is very critical.

How could an increase of temperature above 37 °C alter this subtle balance in patients? It has been shown that the T1620M *SCN5A* mutation found in patients with "classical" BrS alters the temperature sensitivity of fast inactiva-

tion of these channels [17]. However, our study suggests that in patients carrying a *SCN5A* mutation at the heterozygous state in whom the function of mutant channels is either reduced or abolished, the temperature-dependent properties of WT I_{Na} itself might also lead to the typical ECG characteristics during fever. This concept is supported by the observation that the patient with the R535X mutation (channels yielding no measurable current) and the patient with the L325R mutation (channels mediating only a small I_{Na}) both exhibited sensitivity to fever. Moreover, the investigation of the L325R channel properties at different temperatures was not consistent with a mutation specific effect of temperature that would lead to a further decrease of mutant I_{Na}. In consequence, we postulate that the effect of elevated temperature on the remaining I_{Na}, which is mainly or totally mediated by WT channels, could be responsible for the ECG phenotype in BrS patients. Fig. 4 illustrates that the effects of increasing the temperature on WT I_{Na} are multiple and intricate, suggesting that distinct temperature sensitivities govern the different state transitions of the sodium channel (e.g., activation and inactivation). As supported by the simulations presented in Fig. 5, this complex temperature-dependence of WT I_{Na} might then be crucial in determining the balance of currents during depolarization and during the phase 1 of the AP. During phase 1, most of I_{Na} has undergone fast inactivation and only a small fraction of I_{Na} is still contributing to depolarization. Although small, our simulations indicate that this fraction is nonetheless critical. Therefore, accelerated inactivation under conditions of elevated temperature, combined with a decreased level of expression of $Na_v1.5$ channels, might then be sufficient to obliterate the "phase 1 depolarization reserve" and to shift the delicate balance of currents in favour of a premature repolarization, thus revealing a BrS phenotype. This hypothesis is supported by a recent model study by Gima and Rudy who demonstrated that the accelerated inactivation of the T1620M $Na_v1.5$ channel leads to a BrS ECG phenotype through a decreased I_{Na} [16]. However, since the differences in WT I_{Na} properties measured at 37 and 42 °C were minimal (Table 1), one should be cautious in extrapolating our experimental data to the situation of BrS patients with fever. Furthermore, the influence of elevated temperature on the AP is complex and the role of fever in BrS is likely to be multifactorial. It is plausible that temperature-dependent changes of currents other than I_{Na} could precipitate the BrS during fever. For example, fever may also increase the peak transient outward current (I_{to}) through mechanisms similar to those we propose for I_{Na} and precipitate repolarization in epicardial tissue. It was beyond the scope of this study to introduce temperature-dependent kinetics for currents other than I_{Na} and we are aware that this represents a limitation of the model; however, it allows us to demonstrate that the mechanism we propose may be a realistic option that remains to be explored further.

4.3. Misfolding of Na$_v$1.5 protein contributes to the L325R phenotype

The consequences of the BrS *SCN5A* mutations on Na$_v$1.5 function are multiple [1]. Recently, Chahine's group reported three BrS *SCN5A* missense mutations leading to a charge modification and generating channels that were not trafficked to the membrane [24–26]. The L325R mutation described here leads to a similar phenotype since the protein expression was not altered (Fig. 3A) and treatments with chemical chaperones, as well as expression at 28 °C, partially rescued I_{Na}. Misfolding of Na$_v$1.5 therefore appears to be one of the mechanisms underlying BrS, as it is the case for K$_v$LQT1 and hERG channels in congenital long QT syndrome [27], and CFTR channels in cystic fibrosis [21]. The significant mutant I_{Na} increase obtained by treating the cells with curcumin may be of clinical importance since this drug has a very low toxicity profile and has already been tested in a clinical setting as an anti-cancer drug [28]. In contrast, thapsigargin, which similarly to curcumin can block the endoplasmic reticulum Ca^{2+}-pump, did not rescue the mutant I_{Na}. It may therefore be possible that the positive effect of thapsigargin is restricted for specific channels [23].

4.4. Dominant negative effect of mutant Na$_v$1.5

A dominant negative effect of mutant ion channel subunits has been frequently reported for channels formed by multiple α-subunits, such as the K$_v$LQT1 channel in LQTS [29]. In contrast, Na$_v$1.5 is not known to oligomerize with other α-subunits in order to form a minimal ion channel, and, therefore, the dominant negative effect of L325R channels on WT Na$_v$1.5 (Fig. 6B) was unexpected. It can be postulated that mutant proteins interfere directly or indirectly with either biosynthesis or trafficking of WT channels. It also remains to be shown whether this mechanism could be generalized to other mistrafficked BrS channels since, to our knowledge, no study directly addressed this issue.

5. Conclusions

In the past few years, a number of case reports described that fever triggers the clinical manifestations of BrS. Hence, based on these studies and the present work, BrS should be considered in any patient with syncope during febrile state. The genetic background of BrS is heterogeneous. In the small population of fever-susceptible cases presented here, two patients out of four did not carry any mutation in *SCN5A*. Additional investigations are therefore needed to identify the genetic bases of this disorder. Finally, as illustrated by our findings, the molecular and cellular mechanisms underlying the fever-dependent manifestations of BrS are complex. Further studies are needed in order to elucidate this important issue since there is no curative treatment available for BrS to date.

References

[1] Antzelevitch C, Brugada P, Brugada J, Brugada R, Shimizu W, Gussak I, et al. Brugada syndrome: a decade of progress. Circ Res 2002;91: 1114–8.

[2] Napolitano C, Rivolta I, Priori SG. Cardiac sodium channel diseases. Clin Chem Lab Med 2003;41:439–44.

[3] Wilde AA, Antzelevitch C, Borggrefe M, Brugada J, Brugada R, Brugada P, et al. Proposed diagnostic criteria for the Brugada syndrome: consensus report. Circulation 2002;106:2514–9.

[4] Antzelevitch C, Brugada R. Fever and Brugada syndrome. Pacing Clin Electrophysiol 2002;25:1537–9.

[5] Madle A, Kratochvil Z, Polivkova A. The Brugada syndrome. Vnitr Lek 2002;48:255–8.

[6] Porres JM, Brugada J, Urbistondo V, Garcia F, Reviejo K, Marco P. Fever unmasking the Brugada syndrome. Pacing Clin Electrophysiol 2002;25:1646–8.

[7] Mok NS, Priori SG, Napolitano C, Chan NY, Chahine M, Baroudi G. A newly characterized SCN5A mutation underlying Brugada syndrome unmasked by hyperthermia. J Cardiovasc Electrophysiol 2003; 14:407–11.

[8] Smith J, Hannah A, Birnie DH. Effect of temperature on the Brugada ECG. Heart 2003;89:272.

[9] Sanchez JM, Kates AM. Brugada-type electrocardiographic pattern unmasked by fever. Mayo Clin Proc 2004;79:273–4.

[10] Wang Q, Li Z, Shen J, Keating MT. Genomic organization of the human SCN5A gene encoding the cardiac sodium channel. Genomics 1996;34:9–16.

[11] Sherman AJ, Shrier A, Cooper E. Series resistance compensation for whole-cell patch-clamp studies using a membrane state estimator. Biophys J 1999;77:2590–601.

[12] van Bemmelen MX, Rougier JS, Gavillet B, Apotheloz F, Daidie D, Tateyama M, et al. Cardiac voltage-gated sodium channel Nav1.5 is regulated by Nedd4-2 mediated ubiquitination. Circ Res 2004;95:284–91.

[13] Clancy CE, Rudy Y. Linking a genetic defect to its cellular phenotype in a cardiac arrhythmia. Nature 1999;400:566–9.

[14] Luo CH, Rudy Y. A dynamic model of the cardiac ventricular action potential: I. Simulations of ionic currents and concentration changes. Circ Res 1994;74:1071–96.

[15] Faber GM, Rudy Y. Action potential and contractility changes in [Na(+)](i) overloaded cardiac myocytes: a simulation study. Biophys J 2000;78:2392–404.

[16] Gima K, Rudy Y. Ionic current basis of electrocardiographic waveforms: a model study. Circ Res 2002;90:889–96.

[17] Dumaine R, Towbin JA, Brugada P, Vatta M, Nesterenko DV, Nesterenko VV, et al. Ionic mechanisms responsible for the electro-cardiographic phenotype of the Brugada syndrome are temperature dependent. Circ Res 1999;85:803–9.

[18] Smits JP, Eckardt L, Probst V, Bezzina CR, Schott JJ, Remme CA, et al. Genotype-phenotype relationship in Brugada syndrome: electrocardiographic features differentiate SCN5A-related patients from non-SCN5A-related patients. J Am Coll Cardiol 2002;40: 350–6.

[19] Murray KT, Anno T, Bennett PB, Hondeghem LM. Voltage clamp of the cardiac sodium current at 37 degrees C in physiologic solutions. Biophys J 1990;57:607–13.

[20] Valdivia CR, Tester DJ, Rok BA, Porter CB, Munger TM, Jahangir A, et al. A trafficking defective, Brugada syndrome-causing SCN5A mutation rescued by drugs. Cardiovasc Res 2004;62:53–62.

[21] Egan ME, Pearson M, Weiner SA, Rajendran V, Rubin D, Glockner-Pagel J, et al. Curcumin, a major constituent of turmeric, corrects cystic fibrosis defects. Science 2004;304:600–2.

[22] Logan-Smith MJ, Lockyer PJ, East JM, Lee AG. Curcumin, a molecule that inhibits the Ca2+-ATPase of sarcoplasmic reticulum but increases the rate of accumulation of Ca2+. J Biol Chem 2001; 276:46905–11.

[23] Egan ME, Glockner-Pagel J, Ambrose C, Cahill PA, Pappoe L, Balamuth N, et al. Calcium-pump inhibitors induce functional surface expression of Delta F508-CFTR protein in cystic fibrosis epithelial cells. Nat Med 2002;8:485–92.

[24] Baroudi G, Pouliot V, Denjoy I, Guicheney P, Shrier A, Chahine M. Novel mechanism for Brugada syndrome: defective surface local-ization of an SCN5A mutant (R1432G). Circ Res 2001;88:E78.

[25] Baroudi G, Acharfi S, Larouche C, Chahine M. Expression and intracellular localization of an SCN5A double mutant R1232W/T1620M implicated in Brugada syndrome. Circ Res 2002; 90:E11–16.

[26] Baroudi G, Napolitano C, Priori SG, Bufalo AD, Chahine M. Loss of function associated with novel mutations of the SCN5A gene in patients with Brugada syndrome. Can J Cardiol 2004;20:425–30.

[27] Gouas L, Bellocq C, Berthet M, Potet F, Demolombe S, Forhan A, et al. New KCNQ1 mutations leading to haploinsufficiency in a general population; defective trafficking of a KvLQT1 mutant. Cardiovasc Res 2004;63:60–8.

[28] Cheng AL, Hsu CH, Lin JK, Hsu MM, Ho YF, Shen TS, et al. Phase I clinical trial of curcumin, a chemopreventive agent, in pa-tients with high-risk or pre-malignant lesions. Anticancer Res 2001; 21:2895–900.

[29] Chouabe C, Neyroud N, Guicheney P, Lazdunski M, Romey G, Barhanin J. Properties of KvLQT1 K+channel mutations in Romano–Ward and Jervell and Lange–Nielsen inherited cardiac arrhythmias. EMBO J 1997;16:5472–9.